COMPUTER METHODS IN APPLIED MECHANICS AND ENGINEERING 16 (1978) 91–100

SPURIOUS REFLECTION OF ELASTIC WAVES IN NONUNIFORM FINITE ELEMENT GRIDS

Zdeněk P. BAŽANT

Department of Civil Engineering, Northwestern University, Evanston, Illinois 60201, USA

Manuscript received 8 November 1977
Revised manuscript received 31 January 1978

Elastic wave propagation in a one-dimensional grid of finite elements whose size if uniform from element to element except at one node is analyzed, using complex variables. It is found that spurious wave reflection, along with an increase of amplitude of the diffracted wave, takes place when a wave passes between two finite elements of different sizes. Spurious reflection is significant only for relatively small wavelengths (less than ten times the size of the larger elements) and is important even for very small differences in element size (10%). If the wave arrives from finite elements of smaller size, the transmitted wave has a larger amplitude than the incident wave although the mean energy flux is less. The consistent mass matrix is found to give much smaller spurious reflections than the lumped mass matrix and to enable resolution of smaller wavelengths. This contrasts with the fact that for numerical stability (and suppression of spurious grid oscillations) the lumped mass matrix is better, and for suppression of wave dispersion a combination of lumped and consistent mass matrices is best. The study is restricted to explicit time-step algorithm, second-order (central) difference formulas, and finite elements with linear spatial expansions. In this case it is found that the time step has negligible effects.

1. Nature of the problem

Spurious wave motions are a basic problem in the dynamic finite element analysis of structures. Certain aspects of the problem such as spurious grid oscillations, numerical stability and wave dispersion have been analyzed rigorously [1–4]. It is also well known that some spurious wave reflecrions occur as an elastic wave transverses the boundary of finite elements of different sizes [1, 5–9]. However, no clear information as to the actual magnitude of this phenomenon seems to exist in the literature. Therefore, a quantitative analysis of these reflections is chosen as the objective of this study. A one-dimensional grid of finite elements whose size is uniform from element to element except at one node is chosen as the idealized situation to be studied. The analysis will be restricted to the lowest order finite elements with linear interpolation functions in space, and to explicit time-integration algorithms.

2. Wave motion of the finite element grid

Consider a homogeneous elastic medium which is subdivided by a rectangular finite element grid whose step changes at the plane $x = 0$ (fig. 1). For $x < 0$ the grid step is h, and for $x > 0$ the grid step is H. A longitudinal harmonic elastic wave arrives in the direction of the x axis. It ought to pass through the plane $x = 0$ without any reflections because the actual elastic medium is homogeneous. However, since the grid step on each side of this place is not the same the appearance of a spurious reflection should be suspected.

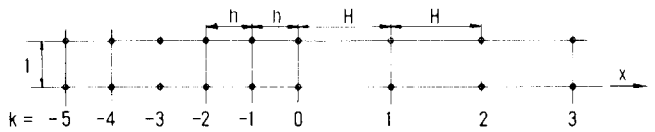

Fig. 1. One-dimensional finite element grid.

Assuming the interpolation (shape) functions of the finite elements to be linear, the elastic nodal forces acting on node k are $-(u_k - u_{k-1})E/h$ from the left and $(u_{k+1} - u_k)E/h$ from the right, where E = Young's elastic modulus, the subscript k indicates the number of the node, and u_k is the displacement of the kth node. While the mass density ρ of the actual elastic medium is uniform, the finite elements may be considered to have a part of their mass density $m\rho$ distributed uniformly throughout each element and the remaining mass density $(1 - m)\rho$ lumped into the nodes. The case $m = 0$ obviously yields the lumped mass matrix, and the case $m = 1$ yields the consistent mass matrix. (The case $m = 0.5$ corresponds to half of the mass being lumped into the nodes, and the case $m = 1.5$ corresponds to all the mass being lumped into the centroid of the element.) The inertia force associated with the lumped mass matrix is $-(1 - m)\rho h\ddot{u}_k$, where superimposed dots are used to denote time derivatives. The inertia forces that correspond to the distributed mass matrix in element $(k - 1, k)$ and derive from $\ddot{u}_k$ and $\ddot{u}_{k-1}$ are triangularly distributed, and their resultants in node k are $m\rho\ddot{u}_k h/3$ and $m\rho\ddot{u}_{k-1}h/3$, respectively. Similar forces result from element $(k, k + 1)$. With all forces put together, the following equations of motion are obtained:

$$\text{for } k < 0: \quad \frac{m}{6}\rho h(\ddot{u}_{k-1} + 4\ddot{u}_k + \ddot{u}_{k+1}) + (1 - m)\rho h\ddot{u}_k = \frac{E}{h}(u_{k+1} - 2u_k + u_{k-1}), \tag{1a}$$

$$\text{for } k = 0: \quad \frac{m}{6}\rho[h(\ddot{u}_{-1} + 2\ddot{u}_0) + H(2\ddot{u}_0 + \ddot{u}_1)] + (1 - m)\rho h_0\ddot{u}_0 = \frac{E}{H}(u_1 - u_0) - \frac{E}{h}(u_0 - u_{-1}), \tag{1b}$$

$$\text{for } k > 0: \quad \frac{m}{6}\rho H(\ddot{u}_{k-1} + 4\ddot{u}_k + \ddot{u}_{k+1}) + (1 - m)\rho H\ddot{u}_k = \frac{E}{H}(u_{k+1} - 2u_k + u_{k-1}), \tag{1c}$$

where $k = 0$ is the node at $x = 0$. Note that the same right-hand sides could be obtained by applying the finite difference method – this is due to the fact that only finite elements with linear interpolation functions are considered.

The numerical integration of the equations of motion of the finite element grid is carried out in time steps τ at the discrete times $t_r = r\tau$, $r = 1, 2, \ldots$. We shall consider those step-by-step time-integration algorithms in which the second time derivatives are replaced by central difference expressions:

$$\ddot{u}_k \approx \frac{1}{\tau^2}(u_{k,r+1} - 2u_{k,r} + u_{k,r-1}). \tag{2}$$

This leads to the usual explicit algorithm for structural dynamics [2]. Other algorithms could be analyzed in a completely analogous manner.

Let the incident wave be $u_k = \exp[i\omega(r\tau - kh/v)]$, in which i = imaginary unit, v = wave velocity and ω = circular frequency = $2\pi v/l$, where l = wavelength. At the dividing node $k = 0$ we must ex-

pect the generation of a reflected wave of amplitude β and a diffracted wave of amplitude γ (this is similar to the arrival of a wave at an interface of two materials [10]). Furthermore, since $k = 0$ is an atypical node of the grid, the amplitude α of its oscillation may also be different. Consequently, we assume the solution to be in the form

$$\text{for } k < 0: \quad u_k = e^{i\omega(r\tau - kh/v)} - \beta e^{i\omega(r\tau + kh/v)} ; \tag{3a}$$

$$\text{for } k = 0: \quad u_0 = \alpha e^{i\omega r\tau} , \tag{3b}$$

$$\text{for } k > 0: \quad u_k = \gamma e^{i\omega(r\tau - kH/V)} , \tag{3c}$$

in which V represents the wave velocity in the finite element grid of step H.

Eqs. (3a)–(3c) may now be substituted in eq. (2) for k, $k - 1$ and $k + 1$, and these may in turn be substituted, along with eqs. (3a)–(3c), into eqs. (1a)–(1c). The exponentials in these equations cancel, and we obtain a system of three linear complex algebraic equations, which may be brought to the form

$$\text{for } k < 0: \quad a_{13}\alpha - (p^2 a_{11} + p a_{12})\beta = -a_{11}/p^2 - a_{12}/p , \tag{4a}$$

$$\text{for } k = 0: \quad a_{22}\alpha - p a_{21}\beta + P a_{23}\gamma = -a_{21}/p , \tag{4b}$$

$$\text{for } k > 0: \quad a_{31}\alpha + (P a_{32} + P^2 a_{33})\gamma = 0 , \tag{4c}$$

in which

$$p = e^{-i\omega h/v} , \qquad P = e^{-i\omega H/V} , \tag{5}$$

$$a_{11} = \frac{2m\psi}{3} + \left(\frac{v_0\tau}{h}\right)^2 , \quad a_{12} = \frac{12 - 4m}{3}\psi - 2\left(\frac{v_0\tau}{h}\right)^2 , \quad a_{13} = a_{11} , \tag{6}$$

$$a_{21} = a_{11} , \quad a_{22} = \frac{12 - 4m}{3}\frac{h_0}{h}\psi - \frac{(v_0\tau)^2}{h}\left(\frac{1}{h} + \frac{1}{H}\right), \quad a_{23} = \frac{2mH}{3h}\psi + \frac{(v_0\tau)^2}{Hh} , \tag{7}$$

$$a_{31} = \frac{2m}{3}\psi + \left(\frac{v_0\tau}{H}\right)^2 , \quad a_{32} = \frac{12 - 4m}{3}\psi - 2\left(\frac{v_0\tau}{H}\right)^2 , \quad a_{33} = a_{31} , \tag{8}$$

$$\psi = \left(\sin\frac{\omega\tau}{2}\right)^2 , \qquad v_0 = \sqrt{E/\rho} . \tag{9}$$

Here v_0 represents the wave velocity in the continuous medium.

Eqs. (4a)–(4c) may be used to solve for the complex amplitudes β and γ of the reflected and transmitted waves.

The special case of $m = 0$ and $\tau = 0$ is analogous to propagation of a wave through the interface between two regular crystal lattices. This problem was solved long ago [11].

3. Relations stemming from propagation through uniform parts of the grid

Before turning attention to the full solution of the foregoing equations it is necessary to formulate certain relations between ψ, τ, v, V, L = wavelength and $\phi = \omega H/V = 2\pi H/L$ which characterize the propagation of the wave along the uniform parts of the finite element grid. Therefore, consider now eq. (4c) alone, which yields

$$a_{31}(e^{i\omega H/V} + e^{-i\omega H/V}) = -a_{32} \,. \tag{10}$$

(As a check, note that eqs. (4a) and (4b) become identical to this relation if $\alpha = \gamma = 1$, $\beta = 0$ and $h = H$.) Substituting for a_{31}, a_{32}, we obtain

$$\cos\phi = \frac{\left(\frac{v_0\tau}{H}\right)^2 - \frac{6-2m}{3}\psi}{\left(\frac{v_0\tau}{H}\right)^2 + \frac{2m}{3}\psi}, \qquad \psi = \left(\sin\frac{\omega\tau}{2}\right)^2 . \tag{11}$$

This equation relates V to L/H and the time step τ. Noting that $V/v_0 = (\omega\tau)(H/v_0\tau)/\phi$, inversion of eq. (11) allows us to deduce

$$\frac{V}{v_0} = \frac{H}{v_0\tau}\frac{2}{\phi}\sqrt{\arcsin\psi}\,, \qquad \psi = \left(\frac{v_0\tau}{H}\right)^2 \frac{1}{\left(\sin\frac{\phi}{2}\right)^{-2} - \frac{2}{3}m} \,. \tag{12}$$

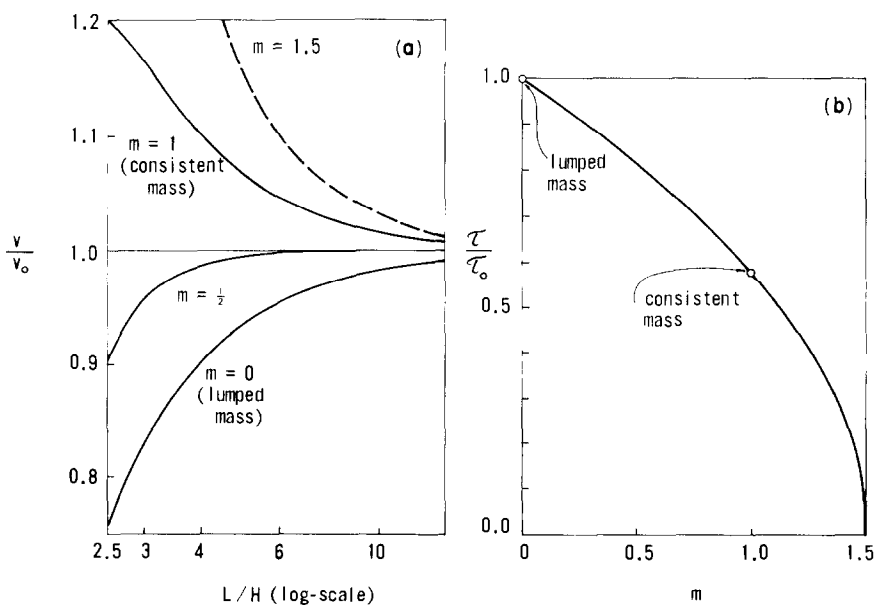

Fig. 2. (a) Wave dispersion due to dependence of wave velocity v on wavelength L (v_0 = wave speed in the continuum), (b) time-step limit for numerical stability.

For a vanishing time step ($\tau \to 0$), i.e. for the exact solution in time this reduces to

$$\frac{V}{v_0} = \frac{2}{\phi}\left[\left(\sin\frac{\phi}{2}\right)^{-2} - \tfrac{2}{3}m\right]^{-1/2}, \quad \phi = \frac{\omega H}{V}, \tag{13}$$

and for $H \to 0$ this yields $V = v_0$.

Eqs. (11)–(13), which will be needed in the subsequent complete solution of eqs. (4a)–(4c), agree with the well-known results on wave dispersion and numerical stability. Eq. (13), plotted in fig. 2, describes the well-known wave dispersion due to the effect of the grid size on wave velocity. No wave propagation is possible (i.e. $V = 0$) when $\phi = 2\pi$ or $L = H$. Note than an increase in m makes V larger (fig. 2). For lumped mass ($m = 0$), V is alwas less than v_0, while for consistent mass ($m = 1$), V is always higher than V_0 (fig. 2). This explains why the consistent mass matrix gives spurious motions ahead of the exact continuum wavefront [7], while the lumped mass matrix does not (and preserved a sharp wavefront).

The condition of numerical stability of the time step algorithm (for $h = H$) is equivalent to the condition that either ω be real of $\mathrm{Im}(\omega) \geqslant 0$ for any L/H. Substituting $V = \omega H/\phi$ into eq. (12), we obtain

$$\left(\sin\frac{\omega\tau}{2}\right)^2 = \psi = \frac{\left(\frac{v_0\tau}{H}\right)^2}{1 - \frac{2m}{3}\left(\sin\frac{\phi}{2}\right)^2}\left(\sin\frac{\phi}{2}\right)^2. \tag{14}$$

To satisfy the stability condition, the right-hand side must obviously be less than or equal to 1 for any ϕ. Thus, it is clear that (for $m = 0$) numerical stability requires that $v_0\tau/H \leqslant 1$ or $\tau \leqslant H/v_0$, as is well known. For $m > 0$ the right-hand side of eq. (14) attains its maximum when $\sin(\phi/2) = 1$, and so numerical stability requires that $(v_0\tau/H)^2 \leqslant 1 - 2m/3$, or

$$\tau \leqslant \tau_0\sqrt{1 - 2m/3}, \quad \tau_0 = \frac{2}{\omega_0}, \quad \omega_0 = \frac{2v_0}{H}, \tag{15}$$

where ω_0 represents the first fundamental frequency of free vibrations of a uniform finite element grid. We see that the numerical stability condition becomes more stringent when m is larger. For a consistent mass matrix ($m = 1$) the limit on τ is one-third of that for the lumped mass. Therefore, from the viewpoint of numerical stability the lumped mass ($m = 0$) is optimum. It is also seen that for numerical stability we must have $m < 1.5$ (thus, all the mass must not be lumped in the centroid).

Numerical stability is usually examined by setting $u_k = a^r \exp[iHK]$ (instead of eq. (3c)) and requiring that $\mathrm{Re}(a) \leqslant 1$. Since $a^r = \exp[r \ln(a)] = \exp[i\omega\tau r]$ for $i\omega\tau = \ln(a)$, the stability condition $\mathrm{Re}(a) \leqslant 1$ is equivalent to $\mathrm{Im}(\omega) \geqslant 0$. Accordingly, the free vibration $u_k = \exp[i\omega\tau r] \times \exp[iHK]$ could be substituted into eq. (1c) – this would yield again eq. (15).

5. Energy flux in the finite element grid

For physical interpretation it is useful to calculate the percentage of the energy flux that is re-

flected. The energy flux to the right represents the power $\mathcal{P}$ (rate of work), which is the product of the nodal force F_k acting on node k from the left and the velocity of the node, i.e. $\mathcal{P} = F_k \dot{u}_k$. When u_k is complex, we must write

$$\mathcal{P} = \mathrm{Re}(F_k)\,\mathrm{Re}(\dot{u}_k)\,. \tag{16}$$

Here F_k is the sum of the elastic force and the inertia force:

$$F_k = -\frac{E}{H}(u_k - u_{k-1}) - \frac{m\rho H}{6}(\ddot{u}_{k-1} + 2\ddot{u}_k)\,, \tag{17}$$

where the inertia term represents the reaction at the node due to the linearly distributed inertia forces within the element. Substituting eq. (17) and $u_k = \gamma \exp[i\xi]$, where $\xi = \omega(t - kH/V) = \omega t - k\phi$, into eq. (16), we get

$$\mathcal{P} = \gamma^2 \omega\left[\frac{E}{H}\left(\frac{1 - \cos\phi}{2}\sin 2\xi + \sin\phi \sin^2\xi\right)\right.$$

$$\left. - \frac{m\rho H}{6}\omega^2\left(\frac{1 + \cos\phi}{2}\sin 2\xi - \sin\phi \sin^2\xi\right)\right]. \tag{18}$$

The time average of $\mathcal{P}$ yields the average energy flux:

$$\langle\mathcal{P}\rangle = \gamma^2 \omega \frac{E}{2H}\left[1 + \frac{m}{6}\left(\frac{\omega H}{v_0}\right)^2\right]\sin\frac{\omega H}{V}\,. \tag{19}$$

This expression is valid for exact integration in time ($\tau \to 0$). For a finite time step the rate of work cannot be defined exactly, but eq. (19) still represents a consistent approximation.

5. Calculation of wave reflection for nonuniform grid

To analyze the wave reflection at $x = 0$ when $h \neq H$, we must calculate amplitudes α, β, γ and the associated powers $\mathcal{P}_\beta$ and $\mathcal{P}_\gamma$ for various chosen values of grid step ratio $H' = H/h$, relative wavelength $L' = L/H$ and relative time step $T' = \tau/T_0 = v_0\tau/H$, where $T_0 = H/v_0$ = time of passage of the wave across the element. The calculation proceeds as follows.

Expressing $\phi = 2\pi/L'$, we may calculate ψ from eq. (12) and evaluate $\omega\tau$ in terms of ψ from eq. (9). Then the relative time step for the grid on the left $\tau' = \tau/(h/v_0)$ is obtained as $\tau' = T'H'$. Solving for ϕ in terms of ψ from eq. (12) and replacing T' with τ' and $\bar{\phi} = \omega h/v = 2\pi h/l$, we obtain

$$\bar{\phi} = 2\arcsin\left[\left(\frac{2m}{3} + \frac{T'^2}{\psi}\right)^{-1/2}\right]. \tag{20}$$

This may be used to evaluate $\bar{\phi}$ (which is the same as ϕ but refers to the grid of step size h rather than H). Subsequently, we may calculate $l' = l/h$ as $l' = 2\pi/\phi'$, as well as $V/v_0 = \omega\tau/\phi T'$ and $v/v_0 = \omega\tau/\bar{\phi}T'H'$. Now we may evaluate $\omega H/V = \omega\tau/(T'V/v_0)$ and $\omega h/v = \omega\tau/(\tau' v/v_0)$ and calculate complex P and p from eq. (5). Then we may evaluate coefficients $a_{11}, a_{21}, \ldots a_{33}$ from eqs. (6)–(8) and solve the system of three algebraic complex eqs. (4). This yields complex amplitudes α, β, γ.

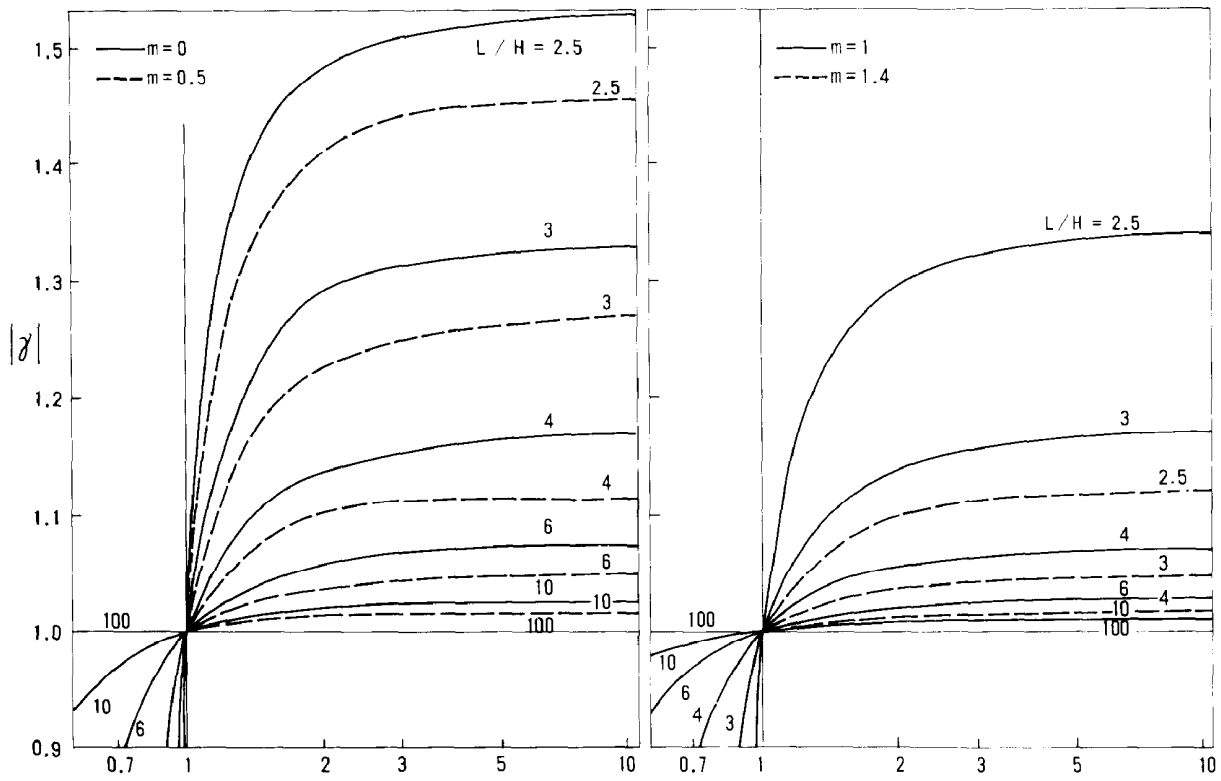

Fig. 3. Amplitude $|\gamma|$ of diffracted wave.

Finally, the ratios of the transmitted and reflected average energy fluxes $\langle \mathcal{P}_\gamma \rangle$ and $\langle \mathcal{P}_\beta \rangle$ to the incident average energy flux $\langle \mathcal{P}_1 \rangle$ may be determined using eq. (19):

$$\frac{\langle \mathcal{P}_\gamma \rangle}{\langle \mathcal{P}_1 \rangle} = \frac{\gamma^2}{H'} \frac{1 + \frac{m}{6}\left(\frac{\omega H}{V}\frac{V}{v_0}\right)^2 \sin\frac{\omega H}{V}}{1 + \frac{m}{6}\left(\frac{\omega h}{v}\frac{v}{V_0}\right)^2 \sin\frac{\omega h}{v}}, \qquad \frac{\langle \mathcal{P}_\beta \rangle}{\langle \mathcal{P}_1 \rangle} = \beta^2 . \tag{21}$$

According to the law of conservation of energy, the sum of these two ratios must equal 1, which serves as a check on the calculations.

The foregoing calculation procedure has been programmed for a computer. The results of the computations are plotted in figs. (3)–(5).

6. Conclusions and analysis of results

From the numerical results the following conclusions may be drawn:

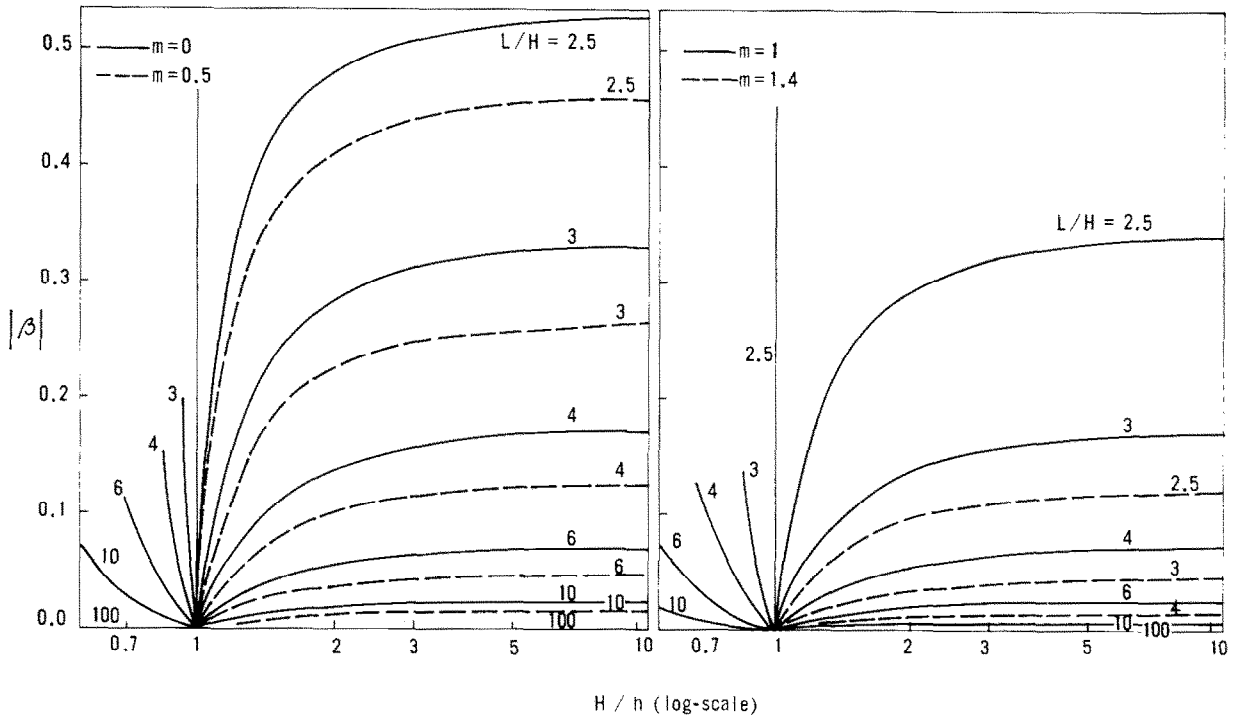

Fig. 4. Amplitude $|\beta|$ of spurious reflected wave.

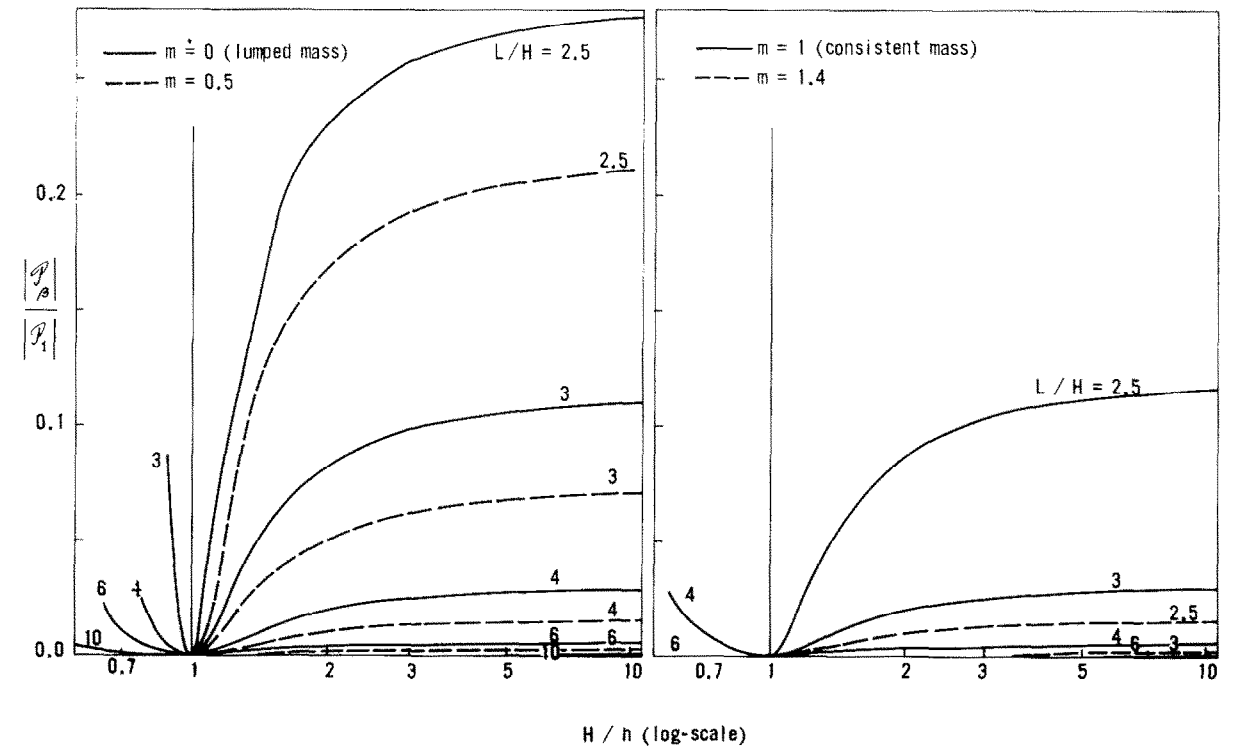

Fig. 5. Energy flux of spurious reflected wave relative to incoming wave.

1. Although elastic waves propagate without reflection in a uniform finite element grid, there is wave reflection when a wave passes between two elements of different sizes (see fig. 1). This reflection is spurious because in a homogeneous continuum which the grid approximates no wave reflection takes place. When explicit algorithms and finite elements with linear expansions in space are considered, it is shown that spurious wave reflection at boundaries of finite elements of different sizes is significant for wavelengths L that are not much greater than the size H of the larger finite element (figs. 3–5). The limit is $L = 10H$ for lumped mass and $L = 6H$ for consistent mass – these values correspond to a reflected wave which is 2.5% of the incident wave in amplitude and 0.1% in average energy flux. Furthermore, at short wavelength the spurious wave reflection is significant even for very small differences in the size of adjacent finite elements (10%; see figs. 3–5). There are only two ways to avoid it – either use a uniform grid or filter out the highest frequencies.

2. If the wave arrives from the finite elements of smaller size, the amplitude of the transmitted wave is larger than that of the incident wave (but the energy flux is of course less) (see fig. 3).

3. The magnitude of the time has a negligible effect on spurious wave reflection. Accordingly, the error due to the central difference operator assumed (2) has no significance in spurious wave reflection. This is however restricted to explicit algorithms: in the case of implicit algorithms this would undoubtedly cease to be true because of the much larger time step. Since the error of the central difference operator is known to balance the error of mass lumping, the comparison might become more favorable to the lumped mass matrix, in the case of implicit algorithms.

4. As far as spurious wave reflections are concerned, the consistent mass matrix is superior to the lumped mass matrix (see case $m = 1$ in figs. 3–5). giving about one-half of the amplitude and one-third of the energy flux for the spurious reflected wave (see case $m = 1$ in figs. 3–5). In other words, the consistent mass matrix allows resolution of shorter wavelengths, which might have been expected from the well-known fact that the consistent mass matrix allows more accurate frequency representation. This advantage of the consistent mass matrix contrasts with the fact that the lumped mass matrix is superior in terms of numerical stability as well as spurious high frequency oscillations of the grid (see fig. 2b), and that for the wave dispersion (due to a change of wave speed in the grid as a function of wavelength) a combination of the lumped mass matrix and the consistent mass matrix is much better than either one of them (see fig. 2a). Consequently, the choice between the lumped mass matrix and the consistent mass matrix is ambiguous and depends on which aspect is more important in the given problem. The cost of computation, which is not discussed here, may often be the major factor.

A few more comments are appropriate. To prevent spurious wave reflection as well as wave dispersion from overshadowing the true dynamic response, it is necessary to eliminate all wavelengths which are less than about 10 times the size of the largest finite element. This may be achieved for example by expanding the applied loads in Fourier series and deleting from the series all high frequency terms. Alternatively, these terms may be filtered out from the response [12].

The present analysis can be easily extended to reflections at the interface of two different materials. For small wavelengths the ratio of finite element sizes on each side of the interface will undoubtedly affect the percentage of the reflected energy flux.

Finally, observe that the conclusion about the effect of the time step does not necessarily hold for implicit algorithms. The present conclusions apply to these algorithms only in the limit for vanishing time step, for which all time-step algorithms converge to the same solution. It is conceivable that the large time steps used in implicit algorithms significantly alter the spurious reflec-

tions. A more detailed analysis of the time step influence on spurious reflection for implicit algorithms is in order since recent experience with unconditionally stable finite time elements has shown that higher order operators exhibit minimal dispersion in nonuniform grids (even without numerical damping) and stabilize the wave response albeit at the cost of some loss in accuracy (private communication by J.H. Argyris, Stuttgart, on results obtained as a sequel to [13]).

References

[1] T.B. Belytschko, Transient analysis, in: Structural mechanics computer programs (Univ. Press of Virginia, Charlottville, VA, 1974) 255–276.
[2] T. Belytschko, N. Holmes and R. Mullen, Explicit integration – stability, solution properties, cost, in: Transient analysis of nonlinear structural behavior (ASME, 1975) 1–21.
[3] M. Fujii, Finite element schemes: stability and convergence, in: J.T. Oden et al. (eds.), Advances in computational methods in structural mechanics and design (Univ. Alabama Press, Alabama, 1972) 201–218.
[4] R.D. Krieg and S.W. Key, Transient shell response by numerical time integration, Int. J. Numer. Meth. Eng. 17 (1973) 273–286.
[5] K.J. Bathe and E.L. Wilson, Stability and accuracy analysis of direct integration methods, Int. J. Earthquake Eng. Struct. Dyn. 1 (1973) 283–291.
[6] K.-J. Bathe and E.L. Wilson, Numerical methods in finite element analysis (Prentice-Hall, Englewood Cliffs, NJ, 1976) ch. 9.
[7] Z.P. Bažant, J.L. Glazik and J.D. Achenbach, Finite element analysis of wave diffraction by a crack, J. Eng. Mech. Div. ASCE 102 (1976) 479–496.
[8] L. Collatz, The numerical treatment of differential equations (Springer, New York, 1966).
[9] R.E. Nickell, Direct integration in structural dynamics, J. Eng. Mech. Div. ASCE 99 (1973) 303–317.
[10] J.D. Achenbach, Wave propagation in elastic solids (North Holland, Amsterdam, 1973).
[11] L. Brillouin, Wave propagation in periodic structures (McGraw Hill, New York, 1946) 85–87, eq. 23.17.
[12] N. Holmes and T. Belytschko, Postprocessing of finite element transient response calculations by digital filters, Computers and structures 6 (1976) 211–216.
[13] J.H. Argyris, L.E. Vaz and K.J. Willam, Higher-order methods for transient diffusion analysis, Comp. Meths. Appl. Mech. Eng. 12 (1977) 243–278.
[14] F.B. Hildebrandt, Finite difference equations and simulations (Prentice-Hall, Englewood Cliffs, NJ, 1968).
[15] W.W. King and J.F. Malluck, Wave diffraction by a crack: finite element simulations, Report (School of Engineering, Georgia Institute of Technology, 1977).